Coordinated Regulation of Nrf2 and Histone H3 Serine 10 Phosphorylation in Arsenite-activated Transcription of the Human Heme Oxygenase-1 Gene

Paul D. Ray[1], **Bo-Wen Huang**[1], and **Yoshiaki Tsuji**[1,2]

[1]Department of Biological Sciences, North Carolina State University, Campus Box 7633, Raleigh, North Carolina 27695-7633

Abstract

Expression of the antioxidant gene heme oxygenase-1 (HO-1) is primarily induced through NFE2-related factor 2 (Nrf2)-mediated activation of the antioxidant response element (ARE). Gene transcription is coordinately regulated by transcription factor activity at enhancer elements and epigenetic alterations such as the posttranslational modification of histone proteins. However, the role of histone modifications in the Nrf2-ARE axis remains largely uncharacterized. The environmental contaminant arsenite is a potent inducer of both HO-1 expression and phosphorylation of histone H3 serine 10 (H3S10); therefore, we investigated the relationships between Nrf2 and H3S10 phosphorylation in arsenite-induced, ARE-dependent, transcriptional activation of the human HO-1 gene. Arsenite increased phosphorylation of H3S10 both globally and at the HO-1 promoter concomitantly with HO-1 transcription in human HaCaT keratinocytes. Conversely, arsenite-induced H3S10 phosphorylation and HO-1 expression was blocked by N-acetylcysteine (NAC), the c-Jun N-terminal kinase (JNK) inhibitor SP600125, and JNK knockdown (siJNK). Interestingly, ablation of arsenite-induced H3S10 phosphorylation by SP600125 or siJNK did not inhibit Nrf2 nuclear accumulation nor ARE binding, despite inhibiting HO-1 expression. In response to arsenite, binding of Nrf2 to the HO-1 ARE preceded phosphorylation of H3S10 at the HO-1 ARE. Furthermore, arsenite-mediated occupancy of phosphorylated H3S10 at the HO-1 ARE was decreased in Nrf2-deficient mouse embryonic fibroblasts. These results suggest the involvement of H3S10 phosphorylation in the Nrf2-ARE axis by proposing that Nrf2 may influence H3S10 phosphorylation at the HO-1 ARE and additional promoter regions. Our data highlights the complex interplay between Nrf2 and H3S10 phosphorylation in arsenite-activated HO-1 transcription.

Graphical abstract

[2]To whom correspondence should be addressed: Yoshiaki Tsuji, Department of Biological Sciences, North Carolina State University, Campus Box 7633, Raleigh, NC 27695., Tel.: 919-513-1106, Fax: 919-515-7169, ytsuji@ncsu.edu.
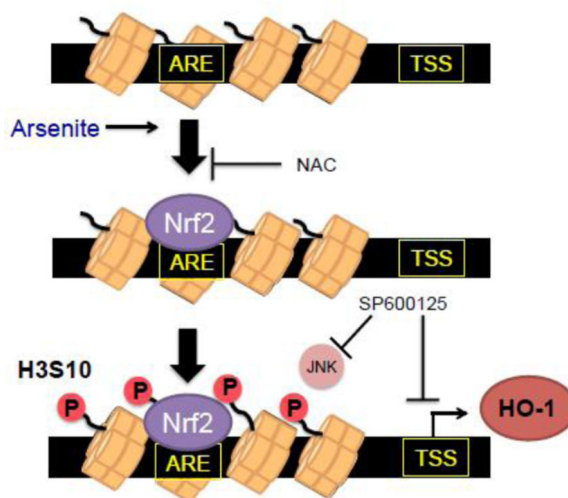
Keywords

Nrf2; histone; epigenetic; arsenic; HO-1; antioxidant response element

1. INTRODUCTION

Arsenic exposure is a major human health concern worldwide [1]. Arsenic is environmentally ubiquitous, and widespread human exposure occurs mainly through contaminated drinking water and is linked to several diseases ranging from diabetes and cardiovascular disorders to cancer [2]. Arsenic produces oxidative stress [2–4], which is associated with the pathogenesis and progression of human disease as a result of reactive oxygen species (ROS)- induced macromolecular damage or aberrant cellular signaling [5, 6]. Oxidative stress has been implicated as a mechanism of action in arsenic-associated disease and so a clearer understanding of the regulation of the cellular antioxidant defense system in arsenic exposure is warranted.

The antioxidant defense system consists of antioxidant factors or enzymes that reduce ROS levels or activity. Heme oxygenase-1 (HO-1) is the primary enzyme in heme catabolism; excess heme is highly toxic, inducing oxidative stress through generation of ROS [7]. HO-1 degrades heme into free iron (Fe^{2+}), carbon monoxide (CO) [8], and biliverdin, which is rapidly converted to the potent antioxidant bilirubin [9]. By regulating intracellular levels of free heme, HO-1 is an essential, highly cytoprotective component of the cellular antioxidant defense system [10]. This is evident in that aberrant expression of HO-1 is implicated in several diseases and morbidity and mortality is observed in HO-1 deficient organisms [11]. HO-1 is highly inducible and many activators of HO-1 expression are pro-oxidants; for example, arsenite, the trivalent form of arsenic, is a potent inducer of HO-1 expression [12, 13]. While arsenite is known to stimulate superoxide anion and H_2O_2 production in a variety of cell lines including immortalized human keratinocytes (HaCaT) [14], the mechanisms of ROS production by arsenite remains elusive.

Transcriptional activation of the HO-1 gene in response to oxidative stress is mediated by the antioxidant response element (ARE) [15, 16]. The ARE is a highly conserved sequence of TGA(C/T)nnnGCA [17] wherein some of the highly conserved bases may not necessarily contribute to transcriptional activation to the degree that the core "n" residues, once thought redundant, do [18]. The ARE binds the NF-E2-related factor 2 (Nrf2) basic-leucine zipper transcription factor and regulates expression of various antioxidant genes [19] to include HO-1 [20]. The upstream promoter region of the HO-1 gene contains several ARE motifs, with the most recognized being the two at −10kb (E2) and −4kb (E1), which are activated by Nrf2 in response to oxidative stress [20, 21]. Cytosolic Nrf2 is bound to the dimeric Kelch-like ECH-associated protein 1 (Keap1)/cullin-3 E-3 ubiquitin ligase (Cul3) inhibitory complex, which promotes continual ubiquitination and proteasomal degradation of Nrf2 [22]. Nrf2 is bound to the Keap1 dimer via two motifs of differing binding affinity and it is generally understood that under oxidative and electrophilic stress conditions, ubiquitination of Nrf2 by Cul3 is prevented possibly through disruption of the low-affinity binding motif between Nrf2 and Keap1, known as the "hinge and latch" model [23]. Stabilized Nrf2 subsequently accumulates and translocates into the nucleus where it forms a heterodimer with small Maf proteins and binds to the ARE [24, 25]. However, a recent study suggests that instead of disrupting contact between Keap1 and Nrf2, electrophilic induction may stabilize Keap1-Nrf2 interaction, yet alters the conformation of Keap1 to prevent Nrf2 ubiquitination [26]. Arsenite may activate the Nrf2-Keap1-ARE axis by direct modification of cysteine residues on Keap1 [27] or by modification of cysteine residues on Nrf2 itself, affecting not only Nrf2-Keap1 binding, but Nrf2 binding to AREs [28].

Regulation of enhancer elements like the ARE in transcription rely not only upon transcription factor activity, but also upon epigenetically mediated changes in the chromatin structure [29]. However, the role of epigenetic alterations in the transcriptional activity of the Nrf2-ARE axis of the HO-1 promoter is understudied. To encapsulate the entire genome into the nucleus, DNA undergoes folding and compaction to form chromatin. The structural unit of chromatin is the nucleosome, a histone octamer composed of the core histones H2A, H2B, H3, and H4, around which DNA is coiled [30]. The N-terminal tails of histones can be post-translationally modified and so regulate gene transcription through chromatin remodeling [31]. While many histone modifications are associated with conventional transcriptional mechanisms, some histone modifications show more molecular specificity in their role as transcriptional regulators, such as the phosphorylation of histone H3 serine 10 (H3S10), which has been associated with the rapid induction of immediate early genes (IEG) such as *c-myc* [32], *c-fos*, and *c-jun* [33–35]. Coactivator proteins have been demonstrated to play a role in ARE activation [36–40]; however, studies revealing relationships between Nrf2 and histone modifications are limited [41]. Arsenite potently induces HO-1 expression and Nrf2 activation, as well as H3S10 phosphorylation [42–44]. This raises the question of whether phosphorylation of H3S10 regulates transcription of HO-1 in response to arsenite, and whether there exists a relationship between the cytoprotective transcription factor Nrf2 and H3S10 phosphorylation.

Employing immortalized human keratinocytes (HaCaT) as a model biologically relevant to arsenite toxicity, our results suggest that arsenite induces HO-1 expression and H3S10

phosphorylation through oxidative stress and Jun N-terminal kinase (JNK)-dependent pathways. Although some histone modifications are understood to provide a platform for transcription factors to bind specific enhancer sequences, we provide evidence suggesting that Nrf2 recruitment to the HO-1 ARE is not dependent on H3S10 phosphorylation, but rather Nrf2 may affect ARE proximal H3S10 phosphorylation. These results suggests that Nrf2 and H3S10 phosphorylation share a critical role in ARE-mediated HO-1 gene activation, which will provide new insight into the regulation of HO-1 in response to environmental exposure to arsenite and other oxidative stressors, as well as providing potential therapeutic targets for arsenicosis.

2. MATERIALS AND METHODS

2.1. Cell Culture and chemical reagents

Immortalized human keratinocyte HaCaT cells [45] were cultured in Dulbecco's Modified Eagle's Medium supplemented with 10% fetal bovine serum (FBS), 100 units/ml penicillin, and 100 ug/ml streptomycin (all from Mediatech). Mouse embryonic fibroblasts (MEF) cultured from wild type and Nrf2-deficient mouse lines [46], a gracious gift from Dr. Jefferson Chan (University of California, Irvine CA), were cultured in Dulbecco's Modified Eagle's Medium supplemented with 0.05uM 2-mercaptoethanol (EMD Millipore), 1mM non-essential amino acids (Mediatech), and 15% FBS. Cells were incubated at 37°C in a humidified 5% carbon dioxide atmosphere. Sodium arsenite ($NaAsO_2$) was purchased from Thermo Fisher Scientific and dissolved in water. The MAPK inhibitors SP600125, SB203580, and U0126 were purchased from Calbiochem and dissolved in DMSO. N-acetyl L-cysteine (NAC) was purchased from Sigma and dissolved in 1M Tris (pH 7.6).

2.2. Antibodies

Antibodies utilized in Western blotting and/or chromatin immunoprecipitation assay (ChIP) were purchased from the following companies: anti-heme oxygenase-1 (sc-7695), anti-Nrf2 (sc-13032X), anti-JNK (sc-571), normal rabbit IgG (sc-2027), normal mouse IgG (sc-2025), and anti-RNAPII (sc-899X) all from Santa Cruz Biotechnology; anti-lamin B (Ab-1) from Oncogene; anti-lactate dehydrogenase (AB1222) from Chemicon; phospho-specific antibodies of p38 MAPK (9211), MEK1/2 (9121), JNK (4688), ERK1/2 (9911), histone H3S10 (3377), and anti-Histone H3 (9715) all from Cell Signaling Technology; ChIP grade phospho-specific anti-H3S10 (ab14955), anti-RNAPIISer2 (ab5095), and anti-RNAPIISer5 (ab5131) from Abcam; and anti-β-actin (A5441) from Sigma.

2.3 Whole cell extracts, nuclear and cytoplasmic fractionation, and Western blotting

Whole cell extracts (WCE) were prepared by lysing cells with lysis buffer (150mM NaCl, 10mM Na_2HPO_4, 1% Triton-X, 0.5% deoxycholic acid, 0.1% sodium dodecyl sulfate (SDS), and 0.2% sodium azide; pH 7.4). Nuclear and cytoplasmic extracts were prepared using a nuclear extraction kit (Active Motif) according to manufacturer's protocol. Cell lysates were electrophoretically separated on SDS-polyacrylamide gels then transferred to polyvinylidene difluoride (PVDF) membranes (Thermo Fisher Scientific) and probed with primary antibodies. After overnight incubation at 4°C, membranes were washed and incubated at room temperature with horseradish peroxidase-conjugated secondary antibody

(CalBiochem) and subsequently incubated in chemiluminescent HyGlo reagent and visualized by exposure to x-ray film (Denville Scientific). Quantification of Western blot signals was conducted by densitometric analysis with Image J software [47]. Relative density of each treatment signal band was normalized to untreated control signal band. Subsequently, normalized relative density of signals was further adjusted by normalization to relative density of loading control signal bands.

2.4 Northern blotting

Total RNA was isolated with TRI Reagent RT (Molecular Research Center) according to manufacturer's protocol. 5–10μg of total RNA was separated on 1.1% agarose gel with 5% formaldehyde in 3-(N-morpholino)-propanesulfonic (MOPS) acid buffer, followed by overnight capillary transfer to a Protran® BA85 nitrocellulose transfer membrane (Whatman). ^{32}P-labeled human heme oxygenase-1 cDNA probe was prepared with MegaPrime DNA Labeling Kit (GE Healthcare) and hybridized with membrane at 42°C overnight and washed with buffer (0.1% SDS in 0.5× SSC buffer) at 52°C. The dried membranes were subjected to autoradiography and visualized on x-ray film. Staining RNA with ethidium bromide was used for equal RNA loading as well as RNA size markers 28S and 18S ribosomal RNA. Quantification of Northern blot signals was conducted by densitometric analysis with Image J software [47]. Relative density of each treatment signal band was normalized to untreated control signal band. Subsequently, normalized relative density of signals was further adjusted by normalization to relative density of loading control signal bands.

2.5 Total ROS detection

HaCaT cells were plated in 24-well plates (Cellstar, Greiner bio-one) in standard culture conditions overnight. Cells were treated with arsenite (10μM) for 2, 4, and 6 hours and incubated with 10μM of CM-H$_2$DCF-DA (2′, 7′-dichlorofluorescein acetate, Life Technologies) dissolved in HBSS for 30 minutes at 37°C in the dark. After incubation with the dye, cells were washed with PBS twice, and fluorescence measured by microplate reader (FLUOstar Omega, BMG LABTECH). The signal was excited at 485 nm, and emission was collected at 520 nm. Fluorescent signal were analyzed with the MARS Data Analysis software (BMG LABTECH).

2.6 Small interfering RNA (siRNA) transfection

100 pmol of siJNK, (Hs_MAPK8_13, sense 5'-CCAGUAAUAUAGUAGUAAATT-3', anti-sense 5'-UUUACUACUAUAUUACUGGGC-3'; Qiagen) or non-targeting siControl (D-001210-01, sense 5'-UAGCGACUAAACACAUCAAUU-3', anti-sense 5'-UUGAUGUGUUUAGUCGCUAUU-3'; Dharmacon) was mixed with 10μl Lipofectamine RNAiMAX (Invitrogen) in 800μl FBS/antibiotic-free OptiMEM (Invitrogen) medium containing sodium bicarbonate. The resulting RNA-lipid complexes were incubated at room temperature for 20 min. The growth media of either 4×10^6 cells in 100-mm dishes, or 2×10^6 cells in 60-mm dishes was removed and replaced with OptiMEM. 400 μl of Lipofectamine/siRNA mix was added to each 100-mm dish (50 pmol), or 200μl was added to each 60-mm dish (25 pmol) and incubated for 6 hours, after which time the OptiMEM/

siRNA mixture was removed and replaced with serum-free DMEM. 48 hours later cells were treated with arsenite and harvested for Western, Northern blotting, and/or ChIP assays.

2.7 ChIP assay and quantitative real time PCR (RT-PCR)

Chromatin immunoprecipitation (ChIP) assay was carried out according to the "Fast ChIP" protocol [48]. Briefly, HaCaT cells transfected with siRNA or treated with arsenite were subjected to chromatin cross-linking with 1.42% formaldehyde, subsequently quenched with 125 mM glycine, and lysed according to the protocol. Cell lysates were sonicated for 12 cycles (12 seconds on; 20 seconds rest) to shear chromatin DNA. Sonicated lysates were subjected to chromatin immunoprecipitation by incubating with control IgG or applicable target antibodies at 4°C in a chilled sonication bath (Branson 2510, 40mHz) for 15 min and then incubated with protein A agarose/ssDNA bead slurry (Millipore 16–157) for 45 minutes. After washing and decrosslinking, the isolated genomic DNA was subjected to SYBR Green qPCR with iQ™ SYBR® Green Supermix (Bio-rad) by using the primer pairs flanking the HO-1 E2 ARE, E1 ARE, transcription start site (TSS), and Exon 3 as previously described [36]. The relative efficiency of each primer set was determined using input genomic DNA. Immunoprecipitated genomic DNA in each sample was normalized to input (C_t), then normalized to control samples and presented as fold enrichment.

3. RESULTS

3.1. Arsenite induces H3S10 phosphorylation and Nrf2 binding at the HO-1 ARE

To address whether histone H3S10 phosphorylation is involved in ARE activation of the human HO-1 gene, we first analyzed induction of HO-1 expression and global phosphorylation of H3S10 in response to arsenite. HaCaT human keratinocytes exposed to 0–25 μM arsenite for 8 hr (Fig. 1a), or 10 μM for 0–24 hr (Fig. 1b), showed increased expression of HO-1 mRNA and protein in a dose and time dependent manner. Global H3S10 phosphorylation occurred concomitantly and followed a similar profile of induction as HO-1 in a dose and time dependent manner (Fig. 1c and d). HO-1 mRNA expression and phosphorylation of H3S10 were increased as early as 4 hr (Fig. 1b and d).

To test whether H3S10 phosphorylation is induced at the HO-1 ARE region during transcriptional activation, HaCaT cells treated with 10 μM arsenite for 4 hr were analyzed by ChIP assay using antibodies specific for phosphorylated H3S10, Nrf2, RNA polymerase II (RNAPol), and RNAPol phosphorylated at serine 2 (RNAPolS2) and serine 5 (RNAPolS5), markers for active transcription. We employed primer sets covering the most recognized ARE regions, the ARE E2 (−10kb ARE) and ARE E1 (−4kb ARE) in addition to the transcription start site (TSS) and the exon 3 region (5 kb downstream from TSS) of the human HO-1 gene (Fig. 2). Transcriptional activation of the HO-1 gene was inferred by Nrf2 binding to the E2 and E1 ARE enhancers (Fig. 2a) and recruitment of RNAPol II to the TSS after arsenite treatment (Fig. 2b). Localization at the TSS and Exon 3 regions of both the elongating RNAPolS2 (Fig. 2c) and initiated RNAPolS5 (Fig. 2d) was increased, further suggesting an active transcriptional state of the HO-1 gene. In contrast to the enrichment of Nrf2, phosphorylation of H3S10 occurred at all assessed regions (Fig. 2e).

3.2 Induction of H3S10 phosphorylation and HO-1 transcription by arsenite in an oxidative stress-dependent manner

To determine whether arsenite induces oxidative stress in our model, HaCaT cells were treated with 10 μM arsenite for 2–6 hr and subjected to ROS detection via fluorescent CM-H$_2$DCF-DA dye. As reported previously [4, 12], production of ROS was induced over 4 fold after 4 hr arsenite treatment (Fig. 3a), suggesting induction of oxidative stress. We next asked whether arsenite induces H3S10 phosphorylation through an oxidative stress-dependent pathway. To this end, we employed the antioxidant N-acetyl L-cysteine (NAC) to test the effect of altered cellular redox status on arsenite-induced phosphorylation of histone H3S10. H3S10 phosphorylation in response to 10 and 30 μM arsenite was blocked by pretreatment with NAC (Fig. 3b). NAC pretreatment also decreased HO-1 protein and mRNA expression (Fig. 3b) in response to arsenite treatment. NAC pretreatment also decreased arsenite-induced nuclear accumulation of Nrf2, a pre-requisite for Nrf2-ARE binding (Fig. 3c). To ascertain whether NAC inhibits induction of phosphorylated histone H3S10 at the HO-1 ARE and promoter regions, HaCaT cells pre-treated with NAC and then exposed to arsenite were subjected to ChIP assay for the E1 ARE (Fig. 3d) and the transcription start site (TSS) (Fig. 3e) of the HO-1 gene. We found that arsenite-induced phosphorylation of histone H3S10 at the HO-1 E1 and TSS regions was decreased by pretreatment with NAC (Fig. 3d and 3e). Induction of Nrf2 binding to the HO-1 E1 and TSS in response to arsenite was also decreased by NAC (Fig. 3d and 3e). Collectively, these results suggest that arsenite-induced oxidative stress is involved in the increase of HO-1 mRNA and protein expression, Nrf2 nuclear accumulation and binding to the HO-1 ARE, and global as well as HO-1 ARE-localized phosphorylation of histone H3S10.

3.3 Regulation of H3S10 phosphorylation by MAPK in response to arsenite

To investigate the protein kinase responsible for arsenite-induced H3S10 phosphorylation, we tested the possible involvement of the oxidative stress-responsive MAPK family members [49, 50]. We first confirmed that arsenite treatment increased levels of phosphorylated p38, ERK, and JNK in HaCaT cells (Fig. 4a). Next, HaCaT cells were pretreated with pharmacological inhibitors of either p38 (SB203580), ERK (U0126), or JNK (SP600125) for 1 hr prior to arsenite treatment. As shown in Fig. 4b, SP600125 decreased arsenite-induced global H3S10 phosphorylation, while U0126 and SB203580 had only marginal effects, suggesting the involvement of the JNK pathway in the phosphorylation of H3S10 by arsenite. Additionally, SP600125 also blocked arsenite-induced HO-1 mRNA and protein expression (Fig. 4c).

Next we explored the possibility that the JNK inhibitor may decrease arsenite-mediated HO-1 expression and H3S10 phosphorylation by blocking the nuclear accumulation of Nrf2; however, the effect of SP600125 on arsenite-induced Nrf2 nuclear accumulation was marginal (Fig. 5a). To further characterize the status of HO-1 promoter elements with regards to phosphorylation of H3S10, Nrf2 binding, and involvement of the JNK pathway, ChIP assays for the E1 ARE and the TSS regions of the HO-1 gene were conducted with HaCaT cells pretreated with SP600125 prior to arsenite challenge for 4 hr. We observed that arsenite-induced phosphorylation of histone H3S10 on the HO-1 E1 and TSS was decreased by pretreatment with SP600125 (Fig. 5b, 5c), while Nrf2 binding to the HO-1 E1 ARE was

not blocked by SP600125 (Fig. 5b). These results suggest that inhibition of histone H3S10 phosphorylation does not affect Nrf2 nuclear accumulation and subsequent binding to the HO-1 AREs. Furthermore, since SP600125 blocked HO-1 mRNA expression induced by arsenite (Fig. 4c) despite having no effect on Nrf2 nuclear accumulation and ARE binding, these results suggest that SP600125 pretreatment inhibits a transcriptional event which occurs after Nrf2 localization to the HO-1 ARE.

3.4 Relationship between H3S10 phosphorylation and Nrf2 in HO-1 ARE activation

We next asked whether JNK is the kinase responsible for the arsenite-induced HO-1 expression and phosphorylation of H3S10. To address this question, we attempted to knockdown JNK in HaCaT cells by employing JNK siRNA and performed Western blotting after treatment with arsenite. When JNK expression was decreased in JNK siRNA-transfected HaCaT cells, increased levels of global H3S10 phosphorylation and HO-1 expression in response to arsenite were decreased (Fig. 6a). However, arsenite-induced Nrf2 nuclear accumulation was not significantly changed after JNK knockdown (Fig. 6a).

Collectively, our results employing NAC (Fig. 3b–e), SP600125 (Fig. 4c, 5a–c), and siJNK (Fig. 6a) led us to ask whether Nrf2 binding to the HO-1 ARE precedes the enrichment of HO-1 ARE with phosphorylated H3S10. A time course ChIP analysis in HaCaT cells treated with arsenite demonstrated that Nrf2 recruitment to the HO-1 ARE was induced almost 5-fold after 30 min of arsenite treatment (Fig. 6b), whereas statistically significant increases in H3S10 phosphorylation at the HO-1 ARE was only detectable after 1 hr (Fig. 6c), suggesting that Nrf2 binding precedes phosphorylation of H3S10 on the HO-1 ARE (Fig. 6d). This profile prompted us to explore the possibility that phosphorylation of histone H3S10 at the HO-1 ARE may be dependent upon Nrf2. To this end, we employed Nrf2 knockout mouse embryonic fibroblasts (MEF) and tested whether Nrf2 deficiency affects H3S10 phosphorylation following arsenite treatment. Increased HO-1 expression and Nrf2 nuclear accumulation by arsenite were significantly decreased in Nrf2−/− MEF cells, though global levels of arsenite-induced H3S10 phosphorylation were unaffected (Fig. 7a). However, we subjected arsenite-treated Nrf2 knockout MEF cells to ChIP assay and observed a loss of not only Nrf2 binding to the HO-1 E1 ARE (Fig. 7b), but also decreased phosphorylated H3S10 at the E1 ARE in Nrf2−/− MEF compared to wild type Nrf2+/+ MEF cells (Fig. 7c). These results suggest that in response to arsenite, Nrf2 may influence H3S10 phosphorylation at the HO-1 promoter during HO-1 transcription, but not total global levels of H3S10 phosphorylation.

4. DISCUSSION

Cells are in a continual battle against oxygen radicals. ROS, while at low levels beneficial signaling molecules [5], in excess engage in constant action against cellular macromolecules. Cellular antioxidant responses rely heavily upon antioxidant enzymes, and timely upregulation of these proteins necessitates a high level of control over transcriptional activation. One of the main "control switches" that regulates antioxidant gene expression is the oxidative stress-responsive enhancer element ARE. While activation of the ARE through the transcription factor Nrf2 has been extensively studied [24, 25, 51], little is known about

the contribution of histone modifications in ARE-mediated gene activation. In this study we set out to investigate whether histone H3S10 phosphorylation regulates HO-1 gene expression through the AREs. We demonstrate here that the HO-1 ARE was enriched with phosphorylated H3S10 when the oxidative stress-inducing metalloid arsenite activated transcription of the HO-1 gene (Fig. 2) and interestingly, phosphorylation of H3S10 may be influenced by Nrf2, the primary transcription factor in ARE activation (Fig. 6, 7).

We employed arsenite in immortalized human keratinocytes as a biologically relevant system, given that arsenite induces hyperkeratotic lesions [52] that are implicated as skin cancer precursors, a disease state in which arsenite-induced oxidative stress is implicated. Our results suggest that oxidative stress induced by arsenite appears to be responsible for the induction of H3S10 phosphorylation (Fig. 3). This is supported by previous reports demonstrating the production of superoxide anion by arsenite in HaCaT cells [4, 12], arsenite-mediated generation of ROS through mitochondrial dysfunction, activation of NADH oxidase, and even the direct oxidation of arsenite to arsenate [53]. Arsenite is potent inducer of the Nrf2-ARE axis through the nuclear accumulation of Nrf2 and its subsequent binding to the ARE [54]. Nuclear accumulation of Nrf2 in response to arsenite may occur through stabilization of Nrf2 by inhibition of Keap1/Cul3-mediated Nrf2 ubiquitination through direct modification of Keap1 cysteine residues by arsenite [27], or by arsenite inducing expression of the adaptor protein p62 which sequesters Keap1 in autophagosomes [55]. Our results suggest that activation of the Nrf2-ARE pathway by arsenite is an event temporally upstream of histone H3S10 phosphorylation (Fig. 3b–e, 4c, 5, 6b–d) and that histone H3S10 phosphorylation of the mouse HO-1 promoter in response to arsenite is dependent on the presence of Nrf2 (Fig. 7). One possible explanation for these observations is that Nrf2 may directly or indirectly recruit a H3S10 kinase to the HO-1 ARE, where upon the kinase, associated with chromatin, phosphorylates H3S10. This is not without precedence; it has been demonstrated that transcription factors such as c-myc [56], CREB [57], and Elk1 [58] associate with H3S10 kinases on enhancer regions.

Chromatin remodeling has been demonstrated to play a role in HO-1 expression. In response to oxidative stress, Brahma-related gene 1 (BRG1), an ATPase of the SWI2/SNF2 family, is recruited to enhancer elements [59], co-localizes with Nrf2 to the HO-1 E2 and E1 AREs and facilitates the recruitment of RNAPol II to the HO-1 TSS via formation of a left-handed Z-DNA structure in the area of the HO-1 promoter, strongly suggesting that chromatin remodeling of the HO-1 promoter is essential for formation of the active transcriptional complex [36]. BRG1 formation of Z-DNA to facilitate transcription by RNAPol II recruitment was not evidenced in other ARE genes such as NQO1 [36], suggesting that ARE genes as a whole are not regulated by the same epigenetic alterations, but that activation of each ARE gene is influenced by epigenetic processes specific for that gene.

It should be noted that the core promoter TSS region upon which the transcription apparatus is formed, as well as the exon 3 coding region, displayed increased phosphorylated histone H3S10 enrichment following arsenite treatment (Fig. 2e), although H3S10 phosphorylation enrichment was higher at the HO-1 E1 ARE as compared to the HO-1 TSS in subsequent ChIP experiments utilizing NAC (Fig. 3d & e) and SP600125 (Fig. 5b & c). This broader distribution of histone H3S10 phosphorylation appears to be consistent with the previous

reports showing gene-wide distribution of specific histone modifications [60]. It may be also consistent with the reports demonstrating that H3S10 phosphorylation regulates transcriptional elongation [56, 61], although it is unknown whether increased H3S10 phosphorylation is necessary for efficient elongation in the coding region. Gene-wide H3S10 phosphorylation in response to arsenite suggests complex signaling mechanisms.

H3S10 is phosphorylated by a wide range of protein kinases [62, 63], including PIM1 [56], Aurora B [64], IKK-α [65, 66], MSK1/2 [67], and Rsk2 [68], along with p38 [50] and c-Jun N-terminal kinases (JNK) [49], members of the oxidative stress-responsive mitogen activated protein kinase (MAPK) signaling cascades. Given the role of p38 and JNK pathways in ARE-regulated gene expression [69–71], and the involvement of chromatin remodeling factors in ARE-gene regulation [36, 41, 72, 73], we characterized the involvement of MAPKs, particularly JNK, in H3S10 phosphorylation and HO-1 transcriptional activation following arsenite exposure. Consistently, it has recently been reported that JNK binds various active promoters and is a direct histone H3S10 kinase during stem cell differentiation [49]. In HO-1 ARE activation, we speculate that phosphorylated H3S10 may further recruit or eject specific histone reader/writer complexes and adaptor proteins for setting up a large and fully active Nrf2-ARE complex. This is supported, for instance, by the reports of HP1 dissociation from heterochromatin upon H3S10 phosphorylation [64], and the recruitment of the phospho-serine binding protein 14-3-3 to phosphorylated H3S10 coupled with c-fos and c-jun gene activation [74].

While Nrf2 is known as the primary transcriptional activator of AREs, Bach1 (BTB and CNC homolog 1), a Maf-related transcriptional repressor, has been identified as a basal repressor of HO-1 transcription through the binding of AREs; treatment with arsenite decreases Bach1 occupancy of the AREs prior to substantial binding of Nrf2 and transcriptional activation [44, 75]. Given that we have demonstrated that Nrf2 binding precedes H3S10 phosphorylation of the ARE (Fig. 6d), it is unlikely that Bach1 plays a direct role in H3S10 phosphorylation other than to facilitate Nrf2 binding.

In conclusion, we provide insight into the role of H3S10 phosphorylation in transcriptional regulation of the ARE-regulated HO-1 gene. Arsenite induced H3S10 phosphorylation in an oxidative stress- and JNK-dependent manner that contributed to HO-1 gene transcription. Furthermore, we provide evidence for the role of Nrf2 in histone H3S10 phosphorylation on the ARE, suggesting a novel role for Nrf2 in the activation of ARE. Further investigations to understand the roles of histone modifications and their direct effectors in the regulation of antioxidant genes through the Nrf2-ARE axis will provide concrete targets for the purpose of modulating cellular antioxidant status.

ACKNOWLEDGEMENTS

REFERENCES

1. Naujokas MF, Anderson B, Ahsan H, Aposhian HV, Graziano JH, Thompson C, Suk WA. The broad scope of health effects from chronic arsenic exposure: update on a worldwide public health problem. Environ Health Perspect. 2013; 121:295–302. [PubMed: 23458756]

2. Jomova K, Jenisova Z, Feszterova M, Baros S, Liska J, Hudecova D, Rhodes CJ, Valko M. Arsenic: toxicity, oxidative stress and human disease. Journal of applied toxicology : J. Appl. Tox. 2011; 31:95–107.

3. Huang C, Ke Q, Costa M, Shi X. Molecular mechanisms of arsenic carcinogenesis. Mol Cell Biochem. 2004; 255:57–66. [PubMed: 14971646]

4. Shi H, Hudson LG, Ding W, Wang S, Cooper KL, Liu S, Chen Y, Shi X, Liu KJ. Arsenite causes DNA damage in keratinocytes via generation of hydroxyl radicals. Chem Res Toxicol. 2004; 17:871–878. [PubMed: 15257611]

5. Ray PD, Huang BW, Tsuji Y. Reactive oxygen species (ROS) homeostasis and redox regulation in cellular signaling. Cell Signal. 2012; 24:981–990. [PubMed: 22286106]

6. Holmstrom KM, Finkel T. Cellular mechanisms and physiological consequences of redox-dependent signalling. Nature reviews. Molecular cell biology. 2014; 15:411–421. [PubMed: 24854789]

7. Kumar S, Bandyopadhyay U. Free heme toxicity and its detoxification systems in human. Toxicology letters. 2005; 157:175–188. [PubMed: 15917143]

8. Tenhunen R, Marver HS, Schmid R. The enzymatic conversion of heme to bilirubin by microsomal heme oxygenase. Proc Natl Acad Sci U S A. 1968; 61:748–755. [PubMed: 4386763]

9. Stocker R, Yamamoto Y, McDonagh AF, Glazer AN, Ames BN. Bilirubin is an antioxidant of possible physiological importance. Science. 1987; 235:1043–1046. [PubMed: 3029864]

10. Ferris CD, Jaffrey SR, Sawa A, Takahashi M, Brady SD, Barrow RK, Tysoe SA, Wolosker H, Barañano DE, Dore S, Poss KD, Snyder SH. Haem oxygenase-1 prevents cell death by regulating cellular iron. Nat Cell Biol. 1999; 1:152–157. [PubMed: 10559901]

11. Morse D, Choi AM. Heme oxygenase-1: the "emerging molecule" has arrived. American journal of respiratory cell and molecular biology. 2002; 27:8–16. [PubMed: 12091240]

12. Cooper KL, Liu KJ, Hudson LG. Contributions of reactive oxygen species and mitogen-activated protein kinase signaling in arsenite-stimulated hemeoxygenase-1 production. Toxicol Appl Pharmacol. 2007; 218:119–127. [PubMed: 17196236]

13. Keyse SM, Tyrrell RM. Heme oxygenase is the major 32-kDa stress protein induced in human skin fibroblasts by UVA radiation, hydrogen peroxide, and sodium arsenite. Proc Natl Acad Sci U S A. 1989; 86:99–103. [PubMed: 2911585]

14. Pi J, Qu W, Reece JM, Kumagai Y, Waalkes MP. Transcription factor Nrf2 activation by inorganic arsenic in cultured keratinocytes: involvement of hydrogen peroxide. Exp Cell Res. 2003; 290:234–245. [PubMed: 14567983]

15. Rushmore TH, Morton MR, Pickett CB. The antioxidant responsive element. Activation by oxidative stress and identification of the DNA consensus sequence required for functional activity. J Biol Chem. 1991; 266:11632–11639. [PubMed: 1646813]

16. Prestera T, Talalay P. Electrophile and antioxidant regulation of enzymes that detoxify carcinogens. Proc. Natl. Acad. Sci., USA. 1995; 92:8965–8969. [PubMed: 7568053]

17. Wasserman WW, Fahl WE. Functional antioxidant responsive elements. Proc. Natl. Acad. Sci., USA. 1997; 94:5361–5366. [PubMed: 9144242]

18. Nioi P, McMahon M, Itoh K, Yamamoto M, Hayes JD. Identification of a novel Nrf2-regulated antioxidant response element (ARE) in the mouse NAD(P)H:quinone oxidoreductase 1 gene: reassessment of the ARE consensus sequence. The Biochemical journal. 2003; 374:337–348. [PubMed: 12816537]

19. Chorley BN, Campbell MR, Wang X, Karaca M, Sambandan D, Bangura F, Xue P, Pi J, Kleeberger SR, Bell DA. Identification of novel NRF2-regulated genes by ChIP-Seq: influence on retinoid X receptor alpha. Nucleic Acids Res. 2012; 40:7416–7429. [PubMed: 22581777]

20. Inamdar NM, Ahn YI, Alam J. The heme-responsive element of the mouse heme oxygenase-1 gene is an extended AP-1 binding site that resembles the recognition sequences for MAF and NF-

E2 transcription factors. Biochem Biophys Res Commun. 1996; 221:570–576. [PubMed: 8630002]

21. Alam J, Stewart D, Touchard C, Boinapally S, Choi AM, Cook JL. Nrf2, a Cap'n'Collar transcription factor, regulates induction of the heme oxygenase-1 gene. J Biol Chem. 1999; 274:26071–26078. [PubMed: 10473555]

22. Furukawa M, Xiong Y. BTB protein Keap1 targets antioxidant transcription factor Nrf2 for ubiquitination by the Cullin 3-Roc1 ligase. Molecular and cellular biology. 2005; 25:162–171. [PubMed: 15601839]

23. Tong KI, Padmanabhan B, Kobayashi A, Shang C, Hirotsu Y, Yokoyama S, Yamamoto M. Different electrostatic potentials define ETGE and DLG motifs as hinge and latch in oxidative stress response. Molecular and cellular biology. 2007; 27:7511–7521. [PubMed: 17785452]

24. Nguyen T, Nioi P, Pickett CB. The Nrf2-antioxidant response element signaling pathway and its activation by oxidative stress. J Biol Chem. 2009; 284:13291–13295. [PubMed: 19182219]

25. Sykiotis GP, Bohmann D. Stress-activated cap'n'collar transcription factors in aging and human disease. Sci Signal. 2010; 3:re3. [PubMed: 20215646]

26. Baird L, Lleres D, Swift S, Dinkova-Kostova AT. Regulatory flexibility in the Nrf2-mediated stress response is conferred by conformational cycling of the Keap1-Nrf2 protein complex. Proc Natl Acad Sci U S A. 2013; 110:15259–15264. [PubMed: 23986495]

27. McMahon M, Lamont DJ, Beattie KA, Hayes JD. Keap1 perceives stress via three sensors for the endogenous signaling molecules nitric oxide, zinc, and alkenals. Proc Natl Acad Sci U S A. 2010; 107:18838–18843. [PubMed: 20956331]

28. He X, Ma Q. NRF2 cysteine residues are critical for oxidant/electrophile-sensing, Kelch-like ECH-associated protein-1-dependent ubiquitination-proteasomal degradation, and transcription activation. Molecular pharmacology. 2009; 76:1265–1278. [PubMed: 19786557]

29. Li B, Carey M, Workman JL. The role of chromatin during transcription. Cell. 2007; 128:707–719. [PubMed: 17320508]

30. Kornberg RD, Lorch Y. Twenty-five years of the nucleosome, fundamental particle of the eukaryote chromosome. Cell. 1999; 98:285–294. [PubMed: 10458604]

31. Bhaumik SR, Smith E, Shilatifard A. Covalent modifications of histones during development and disease pathogenesis. Nature structural & molecular biology. 2007; 14:1008–1016.

32. Chadee DN, Hendzel MJ, Tylipski CP, Allis CD, Bazett-Jones DP, Wright JA, Davie JR. Increased Ser-10 phosphorylation of histone H3 in mitogen-stimulated and oncogene-transformed mouse fibroblasts. J Biol Chem. 1999; 274:24914–24920. [PubMed: 10455166]

33. Nowak SJ, Corces VG. Phosphorylation of histone H3: a balancing act between chromosome condensation and transcriptional activation. Trends Genet. 2004; 20:214–220. [PubMed: 15041176]

34. Mahadevan LC, Willis AC, Barratt MJ. Rapid histone H3 phosphorylation in response to growth factors, phorbol esters, okadaic acid, and protein synthesis inhibitors. Cell. 1991; 65:775–783. [PubMed: 2040014]

35. Li J, Gorospe M, Barnes J, Liu Y. Tumor promoter arsenite stimulates histone H3 phosphoacetylation of proto-oncogenes c-fos and c-jun chromatin in human diploid fibroblasts. J Biol Chem. 2003; 278:13183–13191. [PubMed: 12547826]

36. Zhang J, Ohta T, Maruyama A, Hosoya T, Nishikawa K, Maher JM, Shibahara S, Itoh K, Yamamoto M. BRG1 interacts with Nrf2 to selectively mediate HO-1 induction in response to oxidative stress. Mol. Cell. Biol. 2006; 26:7942–7952. [PubMed: 16923960]

37. Ohta K, Ohigashi M, Naganawa A, Ikeda H, Sakai M, Nishikawa J, Imagawa M, Osada S, Nishihara T. Histone acetyltransferase MOZ acts as a co-activator of Nrf2-MafK and induces tumour marker gene expression during hepatocarcinogenesis. Biochem. J. 2007; 402:559–566. [PubMed: 17083329]

38. Katoh Y, Itoh K, Yoshida E, Miyagishi M, Fukamizu A, Yamamoto M. Two domains of Nrf2 cooperatively bind CBP, a CREB binding protein, and synergistically activate transcription. Genes Cells. 2001; 6:857–868. [PubMed: 11683914]

39. Tsuji Y, Moran E, Torti SV, Torti FM. Transcriptional regulation of the mouse ferritin H gene: Involvement of p300/CBP adaptor proteins in FER-1 enhancer activity. J. Biol. Chem. 1999; 274:7501–7507. [PubMed: 10066817]

40. Kim JH, Yu S, Chen JD, Kong AN. The nuclear cofactor RAC3/AIB1/SRC-3 enhances Nrf2 signaling by interacting with transactivation domains. Oncogene. 2013; 32:514–527. [PubMed: 22370642]

41. Sun J, Brand M, Zenke Y, Tashiro S, Groudine M, Igarashi K. Heme regulates the dynamic exchange of Bach1 and NF-E2-related factors in the Maf transcription factor network. Proc. Natl. Acad.Sci., USA. 2004; 101:1461–1466. [PubMed: 14747657]

42. Li B, Li X, Zhu B, Zhang X, Wang Y, Xu Y, Wang H, Hou Y, Zheng Q, Sun G. Sodium arsenite induced reactive oxygen species generation, nuclear factor (erythroid-2 related) factor 2 activation, heme oxygenase-1 expression, and glutathione elevation in Chang human hepatocytes. Environmental toxicology. 2013; 28:401–410. [PubMed: 21809430]

43. He Z, Ma WY, Liu G, Zhang Y, Bode AM, Dong Z. Arsenite-induced phosphorylation of histone H3 at serine 10 is mediated by Akt1, extracellular signal-regulated kinase 2, and p90 ribosomal S6 kinase 2 but not mitogen- and stress-activated protein kinase 1. J Biol Chem. 2003; 278:10588–10593. [PubMed: 12529330]

44. Reichard JF, Motz GT, Puga A. Heme oxygenase-1 induction by NRF2 requires inactivation of the transcriptional repressor BACH1. Nucleic Acids Res. 2007; 35:7074–7086. [PubMed: 17942419]

45. Boukamp P, Petrussevska RT, Breitkreutz D, Hornung J, Markham A, Fusenig NE. Normal keratinization in a spontaneously immortalized aneuploid human keratinocyte cell line. J Cell Biol. 1988; 106:761–771. [PubMed: 2450098]

46. Leung L, Kwong M, Hou S, Lee C, Chan JY. Deficiency of the Nrf1 and Nrf2 transcription factors results in early embryonic lethality and severe oxidative stress. J Biol Chem. 2003; 278:48021–48029. [PubMed: 12968018]

47. Schneider CA, Rasband WS, Eliceiri KW. NIH Image to ImageJ: 25 years of image analysis. Nature methods. 2012; 9:671–675. [PubMed: 22930834]

48. Nelson JD, Denisenko O, Bomsztyk K. Protocol for the fast chromatin immunoprecipitation (ChIP) method. Nat Protoc. 2006; 1:179–185. [PubMed: 17406230]

49. Tiwari VK, Stadler MB, Wirbelauer C, Paro R, Schubeler D, Beisel C. A chromatin-modifying function of JNK during stem cell differentiation. Nat Genet. 2012; 44:94–100. [PubMed: 22179133]

50. Zhong SP, Ma WY, Dong Z. ERKs and p38 kinases mediate ultraviolet B-induced phosphorylation of histone H3 at serine 10. J Biol Chem. 2000; 275:20980–20984. [PubMed: 10806218]

51. Kobayashi A, Ohta T, Yamamoto M. Unique function of the Nrf2-Keap1 pathway in the inducible expression of antioxidant and detoxifying enzymes. Methods in enzymology. 2004; 378:273–286. [PubMed: 15038975]

52. Endo H, Sugioka Y, Nakagi Y, Saijo Y, Yoshida T. A novel role of the NRF2 transcription factor in the regulation of arsenite-mediated keratin 16 gene expression in human keratinocytes. Environ Health Perspect. 2008; 116:873–879. [PubMed: 18629308]

53. Shi H, Shi X, Liu KJ. Oxidative mechanism of arsenic toxicity and carcinogenesis. Mol Cell Biochem. 2004; 255:67–78. [PubMed: 14971647]

54. Reichard JF, Sartor MA, Puga A. BACH1 is a specific repressor of HMOX1 that is inactivated by arsenite. J Biol Chem. 2008; 283:22363–22370. [PubMed: 18550526]

55. Lau A, Zheng Y, Tao S, Wang H, Whitman SA, White E, Zhang DD. Arsenic inhibits autophagic flux, activating the Nrf2-Keap1 pathway in a p62-dependent manner. Molecular and cellular biology. 2013; 33:2436–2446. [PubMed: 23589329]

56. Zippo A, De Robertis A, Serafini R, Oliviero S. PIM1-dependent phosphorylation of histone H3 at serine 10 is required for MYC-dependent transcriptional activation and oncogenic transformation. Nat Cell Biol. 2007; 9:932–944. [PubMed: 17643117]

57. Shimada M, Nakadai T, Fukuda A, Hisatake K. cAMP-response element-binding protein (CREB) controls MSK1-mediated phosphorylation of histone H3 at the c-fos promoter in vitro. J Biol Chem. 2010; 285:9390–9401. [PubMed: 20089855]

58. Drobic B, Perez-Cadahia B, Yu J, Kung SK, Davie JR. Promoter chromatin remodeling of immediate-early genes is mediated through H3 phosphorylation at either serine 28 or 10 by the MSK1 multi-protein complex. Nucleic Acids Res. 2010; 38:3196–3208. [PubMed: 20129940]

59. Cheng SW, Davies KP, Yung E, Beltran RJ, Yu J, Kalpana GV. c-MYC interacts with INI1/hSNF5 and requires the SWI/SNF complex for transactivation function. Nat Genet. 1999; 22:102–105. [PubMed: 10319872]

60. Rando OJ. Global patterns of histone modifications. Curr Opin Genet Dev. 2007; 17:94–99. [PubMed: 17317148]

61. Hartzog GA, Tamkun JW. A new role for histone tail modifications in transcription elongation. Genes & development. 2007; 21:3209–3213. [PubMed: 18079170]

62. Dong Z, Bode AM. The role of histone H3 phosphorylation (Ser10 and Ser28) in cell growth and cell transformation. Molecular carcinogenesis. 2006; 45:416–421. [PubMed: 16637065]

63. Banerjee T, Chakravarti D. A peek into the complex realm of histone phosphorylation. Molecular and cellular biology. 2011; 31:4858–4873. [PubMed: 22006017]

64. Hirota T, Lipp JJ, Toh BH, Peters JM. Histone H3 serine 10 phosphorylation by Aurora B causes HP1 dissociation from heterochromatin. Nature. 2005; 438:1176–1180. [PubMed: 16222244]

65. Yamamoto Y, Verma UN, Prajapati S, Kwak YT, Gaynor RB. Histone H3 phosphorylation by IKK-alpha is critical for cytokine-induced gene expression. Nature. 2003; 423:655–659. [PubMed: 12789342]

66. Anest V, Hanson JL, Cogswell PC, Steinbrecher KA, Strahl BD, Baldwin AS. A nucleosomal function for IkappaB kinase-alpha in NF-kappaB-dependent gene expression. Nature. 2003; 423:659–663. [PubMed: 12789343]

67. Duncan EA, Anest V, Cogswell P, Baldwin AS. The kinases MSK1 and MSK2 are required for epidermal growth factor-induced, but not tumor necrosis factor-induced, histone H3 Ser10 phosphorylation. J Biol Chem. 2006; 281:12521–12525. [PubMed: 16517600]

68. Sassone-Corsi P, Mizzen CA, Cheung P, Crosio C, Monaco L, Jacquot S, Hanauer A, Allis CD. Requirement of Rsk-2 for epidermal growth factor-activated phosphorylation of histone H3. Science. 1999; 285:886–891. [PubMed: 10436156]

69. Yu R, Chen C, Mo YY, Hebbar V, Owuor ED, Tan TH, Kong AN. Activation of mitogen-activated protein kinase pathways induces antioxidant response element-mediated gene expression via a Nrf2-dependent mechanism. J. Biol. Chem. 2000; 275:39907–39913. [PubMed: 10986282]

70. Kietzmann T, Samoylenko A, Immenschuh S. Transcriptional regulation of heme oxygenase-1 gene expression by MAP kinases of the JNK and p38 pathways in primary cultures of rat hepatocytes. J Biol Chem. 2003; 278:17927–17936. [PubMed: 12637567]

71. Zipper LM, Mulcahy RT. Inhibition of ERK and p38 MAP kinases inhibits binding of Nrf2 and induction of GCS genes. Biochem Biophys Res Commun. 2000; 278:484–492. [PubMed: 11097862]

72. Sakamoto K, Iwasaki K, Sugiyama H, Tsuji Y. Role of the tumor suppressor PTEN in antioxidant responsive element-mediated transcription and associated histone modifications. Mol Biol Cell. 2009; 20:1606–1617. [PubMed: 19158375]

73. Huang BW, Ray PD, Iwasaki K, Tsuji Y. Transcriptional regulation of the human ferritin gene by coordinated regulation of Nrf2 and protein arginine methyltransferases PRMT1 and PRMT4. FASEB journal. 2013; 27:3763–3774. [PubMed: 23699174]

74. Macdonald N, Welburn JP, Noble ME, Nguyen A, Yaffe MB, Clynes D, Moggs JG, Orphanides G, Thomson S, Edmunds JW, Clayton AL, Endicott JA, Mahadevan LC. Molecular basis for the recognition of phosphorylated and phosphoacetylated histone h3 by 14-3-3. Mol Cell. 2005; 20:199–211. [PubMed: 16246723]

75. MacLeod AK, McMahon M, Plummer SM, Higgins LG, Penning TM, Igarashi K, Hayes JD. Characterization of the cancer chemopreventive NRF2-dependent gene battery in human keratinocytes: demonstration that the KEAP1-NRF2 pathway, and not the BACH1-NRF2 pathway, controls cytoprotection against electrophiles as well as redox-cycling compounds. Carcinogenesis. 2009; 30:1571–1580. [PubMed: 19608619]

Highlights

- Arsenite induces H3S10 phosphorylation (H3S10-P) and Nrf2 binding at the HO- 1 ARE.

- Both NAC and SP600125 block arsenite-induced HO-1 expression.

- NAC decreases enrichment of H3S10-P and Nrf2 at the HO-1 ARE.

- SP600125 blocks enrichment of H3S10-P but not Nrf2 at the HO-1 ARE.

- Arsenite-induced Nrf2 binding to the HO-1 ARE precedes H3S10-P.

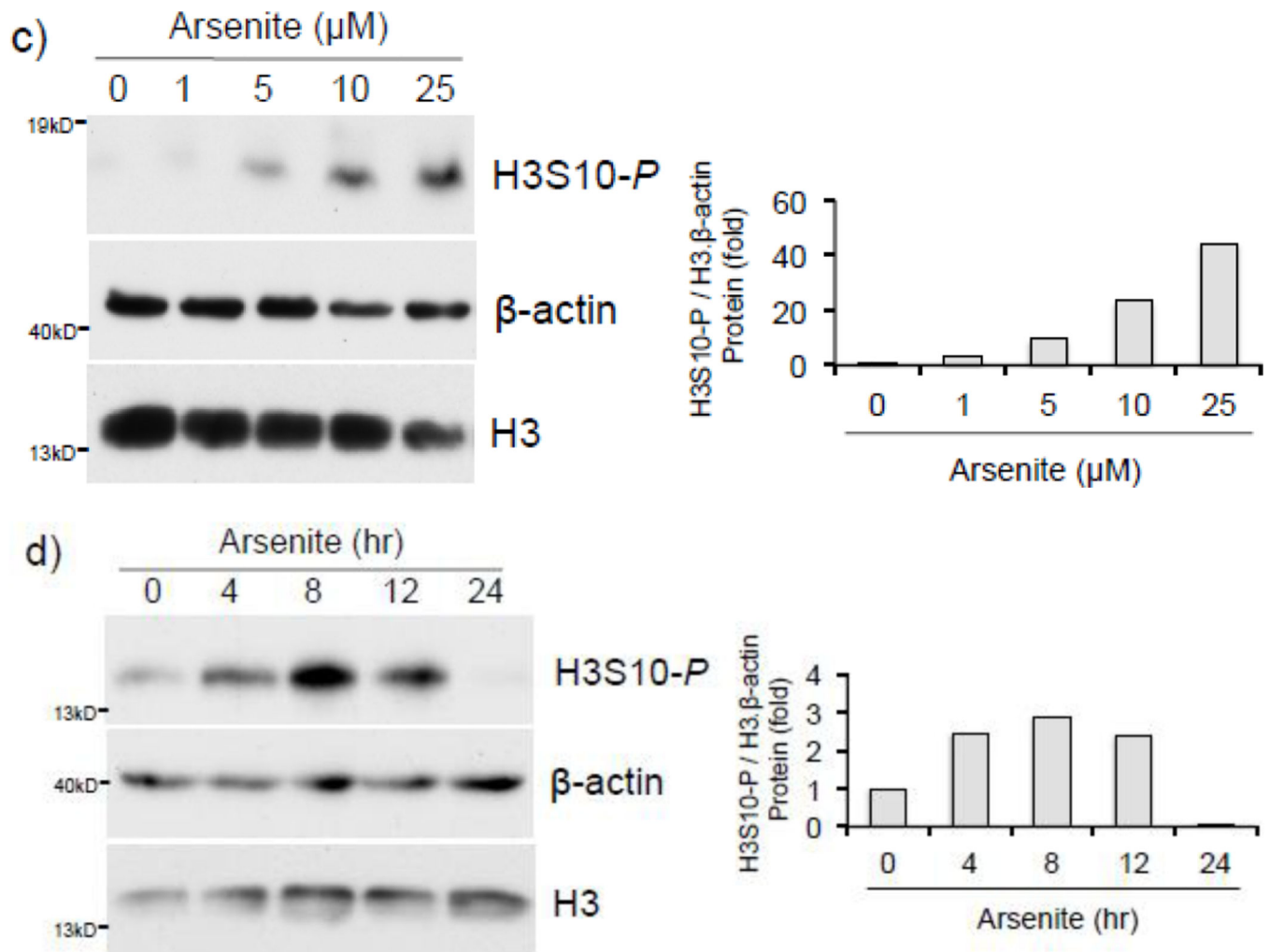- Arsenite-induced H3S10-P at the HO-1 ARE was decreased in Nrf2−/− MEF cells.
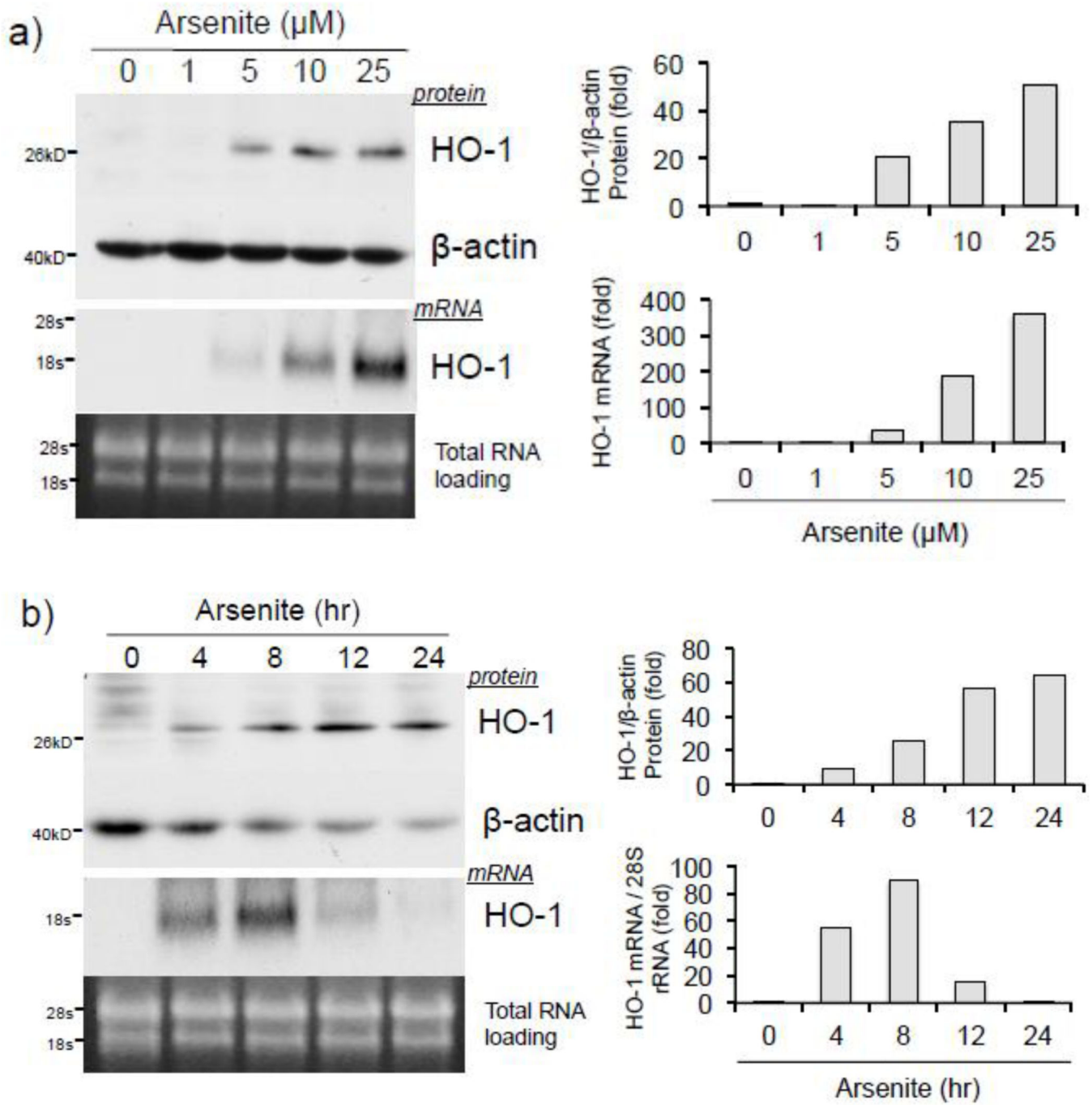
Figure 1. Arsenite induces H3S10 phosphorylation and HO-1 expression
HaCaT cells were treated with 1, 5, 10, or 25μM arsenite for 8 hr (a and c), or alternatively treated with 10μM arsenite for 4, 8, 12, or 24 hr (b and d) and harvested as either whole cell lysate or total RNA. Whole cell lysates were subjected to Western blot analysis with anti-HO-1 and anti-H3S10 phospho-specific (H3S10-P) antibodies; β-Actin and histone H3 blots are shown as loading controls. 6 μg of total RNA was subjected to Northern blot analysis employing a ^{32}P-labeled HO-1 cDNA probe; ethidium bromide staining of total RNA is shown to verify equal loading and positions of 18 and 28S ribosomal RNA are indicated. Quantification of blots is shown to the right. Densitometry analysis was conducted with Image J software. Relative density of arsenite treated signal bands were normalized to the corresponding control signal bands for fold change, then further normalized to the relative density of loading control signal bands for loading accuracy. For HO-1 protein blots, β-Actin signals were used for normalization, while for H3S10-P, the average relative density of β-Actin and histone H3 signal bands were used. The 28s rRNA band was used for normalization of the HO-1 mRNA signal bands.
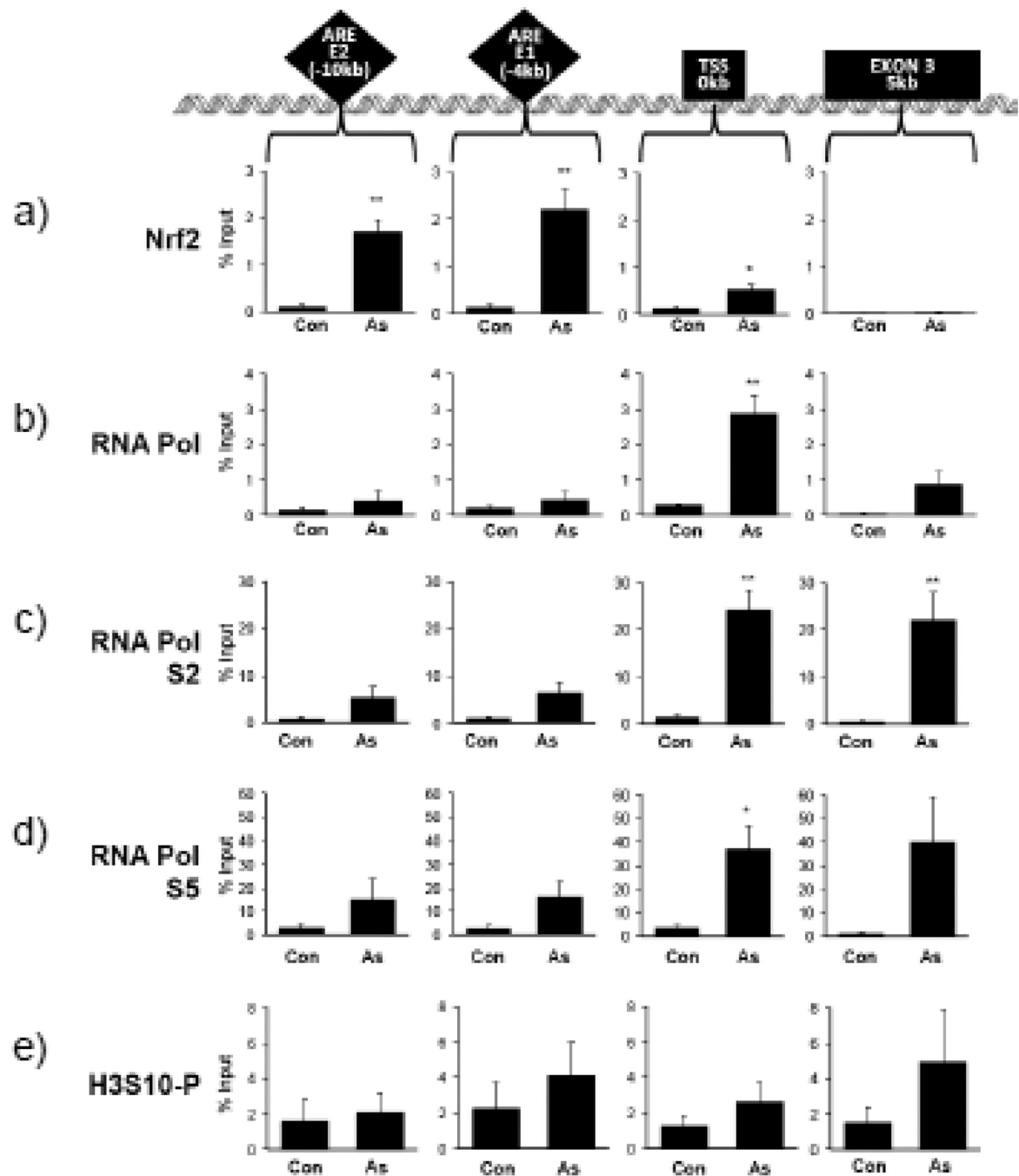
Figure 2. Arsenite induces H3S10 phosphorylation and transcriptional activation of the HO-1 gene

HaCaT cells were treated with 10μM arsenite for 4 hr, then harvested for chromatin immunoprecipitation (ChIP) and incubated with rabbit IgG, anti-Nrf2 (a), anti-RNA Pol II (b), anti-phospho-RNAPol S2 (c), anti-phospho RNAPol S5 (d), or anti-H3S10 phospho-specific (H3S10-P) (e) antibody as described in Materials and Methods. Isolated genomic DNA was subjected to quantitative RT-PCR using primer pairs for the HO-1 E2, E1, TSS, and Exon 3 regions. Samples were normalized to input and presented as percent input.

Significance was calculated using a t-test and established with $p < 0.05$ (*) or $p < 0.01$ (**). A representative of four independent experiments is shown.

a)
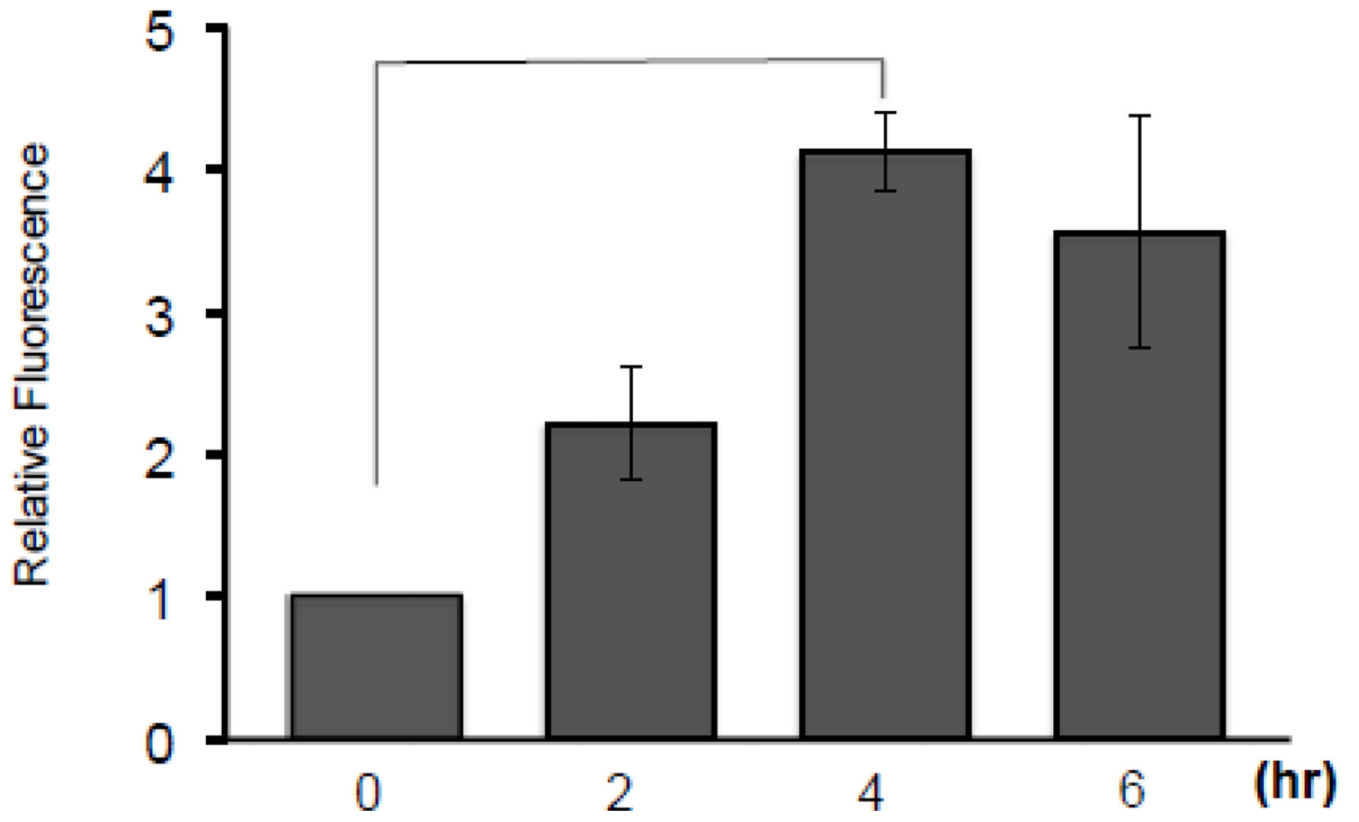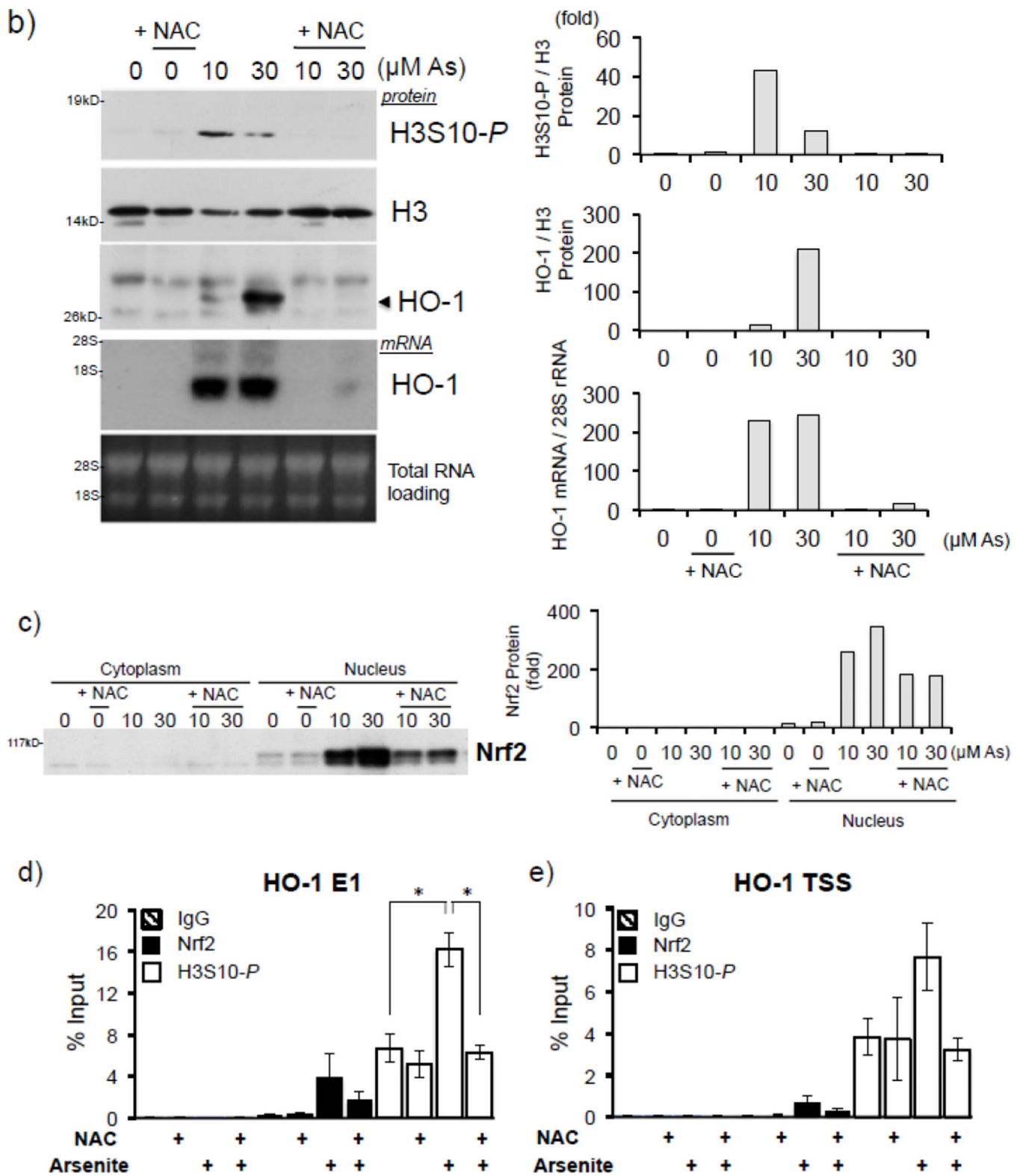
Figure 3. Arsenite induces H3S10 phosphorylation and HO-1 expression through oxidative stress-dependent mechanisms

(a) HaCaT cells were treated with 10μM arsenite for 2, 4, and 6 hr, and then analyzed for total cellular ROS production by CM-H$_2$DCF-DA assay. Fluorescence levels of control cells without arsenite treatment (0) was defined as 1. Significance was calculated using a t-test and established with $p < 0.05$. Results are means ± SE of 4 independents experiments. (b) HaCaT cells were pretreated with 10mM NAC for 1 hr, then treated with 10 or 30μM arsenite for 8 hr and harvested as whole cell lysates or total RNA. Whole cell lysates were subjected to Western blot analysis with anti-HO-1 and anti-H3S10 phospho-specific (H3S10-P) antibodies; histone H3 blot is shown as loading control. 5 μg of total RNA was subjected to Northern blot analysis employing a ^{32}P-labeled HO-1 cDNA probe; ethidium bromide staining of total RNA is shown to verify equal loading and positions of 18 and 28S ribosomal RNA are indicated. (c) In the same condition as (b), nuclear and cytoplasmic extracts were prepared and subjected to Western blot analysis with anti-Nrf2 specific antibody. Quantification of blots in b) and c) is shown to the right. Densitometry analysis was conducted with Image J software. Relative density of arsenite and NAC treated signal bands were normalized to the corresponding control signal bands for fold change, then further normalized to the relative density of loading control signal bands for loading accuracy. For HO-1 and H3S10-P protein blots, H3 signals were used for normalization. The 28s rRNA band was used for normalization of the HO-1 mRNA signal bands. (d & e) HaCaT cells were pretreated with 10mM NAC for 1 hr, then treated with 10μM arsenite for 4 hr and harvested for chromatin immunoprecipitation (ChIP) and incubated with rabbit IgG, anti-H3S10 phospho-specific (H3S10-P), or anti-Nrf2 antibody. Isolated genomic DNA was subjected to quantitative RT-PCR using primer pairs for the HO-1 E1 (d) and TSS (e) regions. Samples were normalized to input and presented as percent input. Significance was calculated using a t-test and established with $p < 0.05$. A representative of three independent experiments is shown.
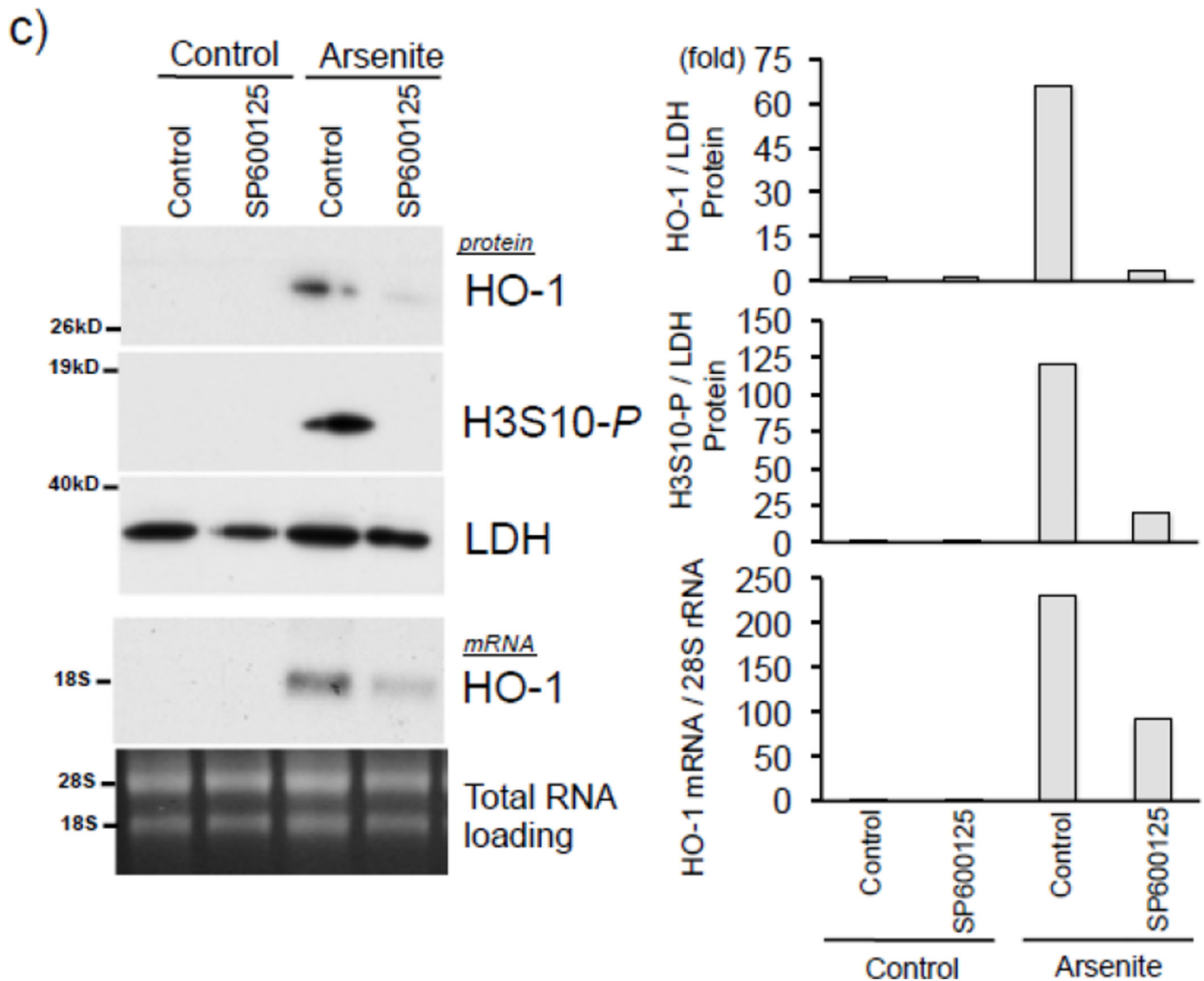
a)

b)
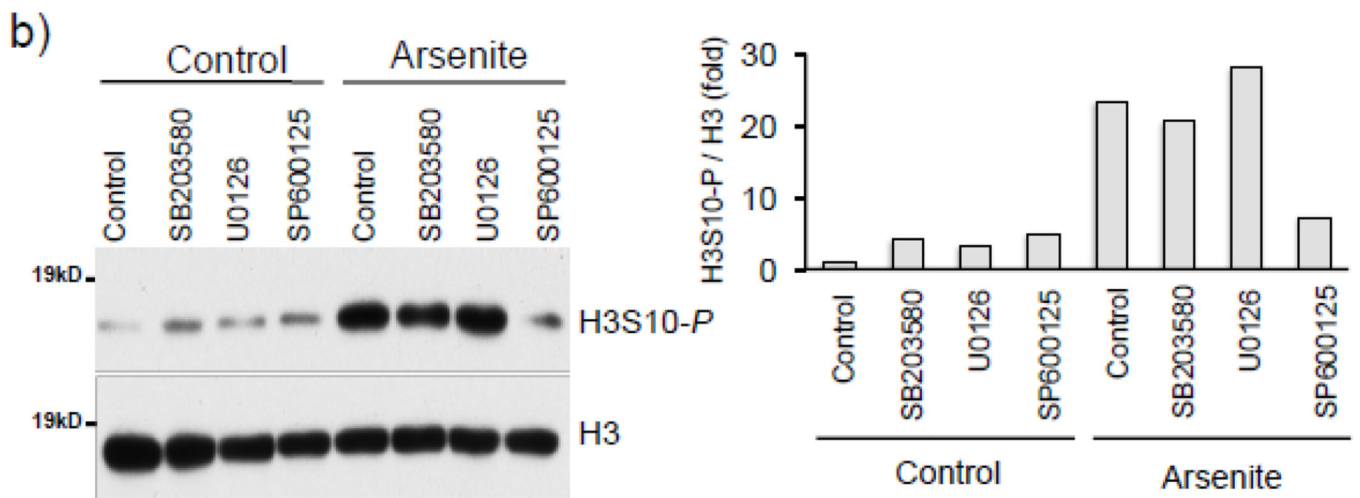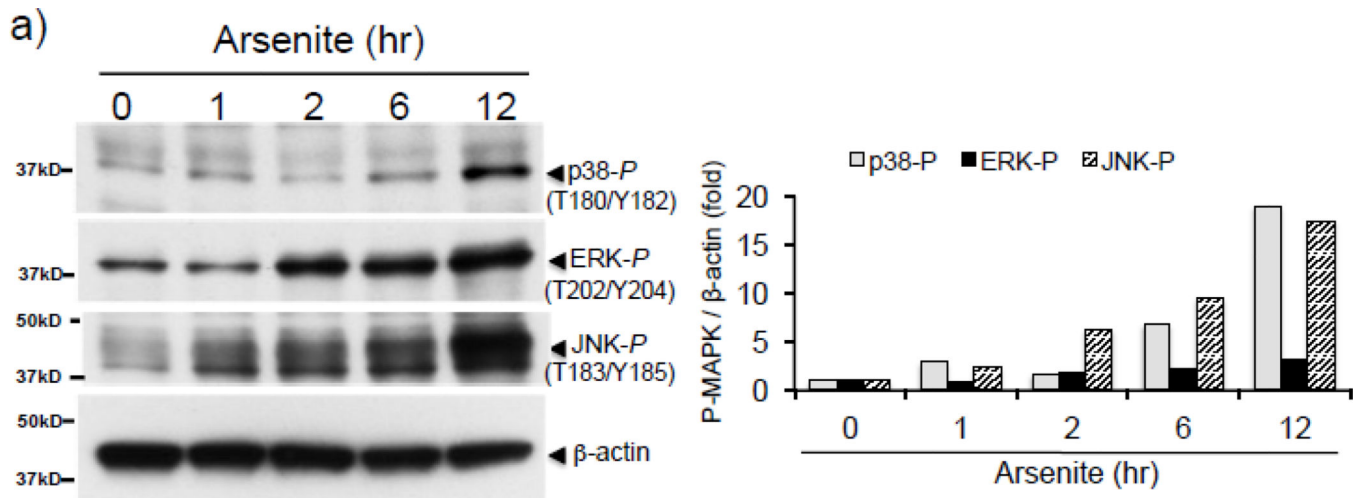
Figure 4. Induction of H3S10 phosphorylation and HO-1 by arsenite is MAPK-dependent
(a) HaCaT cells were treated with 10μM arsenite for 1, 2, 6, or 12 hr and harvested as whole cell lysate and subjected to Western blot analysis with anti-phospho p38 (T180/Y182), anti-phospho ERK (T202/Y204), and anti-phospho JNK (T183/Y185) specific antibodies. (b) HaCaT cells were pretreated with 10μM SB203580, U0126, or SP600125 for 1 hr, then treated with 10μM arsenite for 8 hr. Whole cell lysates were subjected to Western blot analysis with anti-H3S10 phospho-specific antibody; histone H3 blot is shown as loading control. (c) HaCaT cells were pretreated with 10μM SP600125 for 1 hr, then treated with 10μM arsenite for 8 hr and harvested as whole cell lysates or total RNA. Whole cell lysates were subjected to Western blot analysis with anti-HO-1 and anti-H3S10 phospho-specific antibodies; lactate dehydrogenase (LDH) blot is shown as loading control. 7 μg of total RNA was subjected to Northern blot analysis employing a ^{32}P-labeled HO-1 cDNA probe; ethidium bromide staining of total RNA is shown to verify equal loading and positions of 18 and 28S ribosomal RNA are indicated. Quantification of blots is shown to the right. Densitometry analysis was conducted with Image J software. Relative density of arsenite

and SP600125 treated signal bands were normalized to the corresponding control signal bands for fold change, then further normalized to the relative density of loading control signal bands for loading accuracy. β-Actin, H3, and LDH signals were used for protein normalization. The 28s rRNA band was used for normalization of the HO-1 mRNA signal bands.
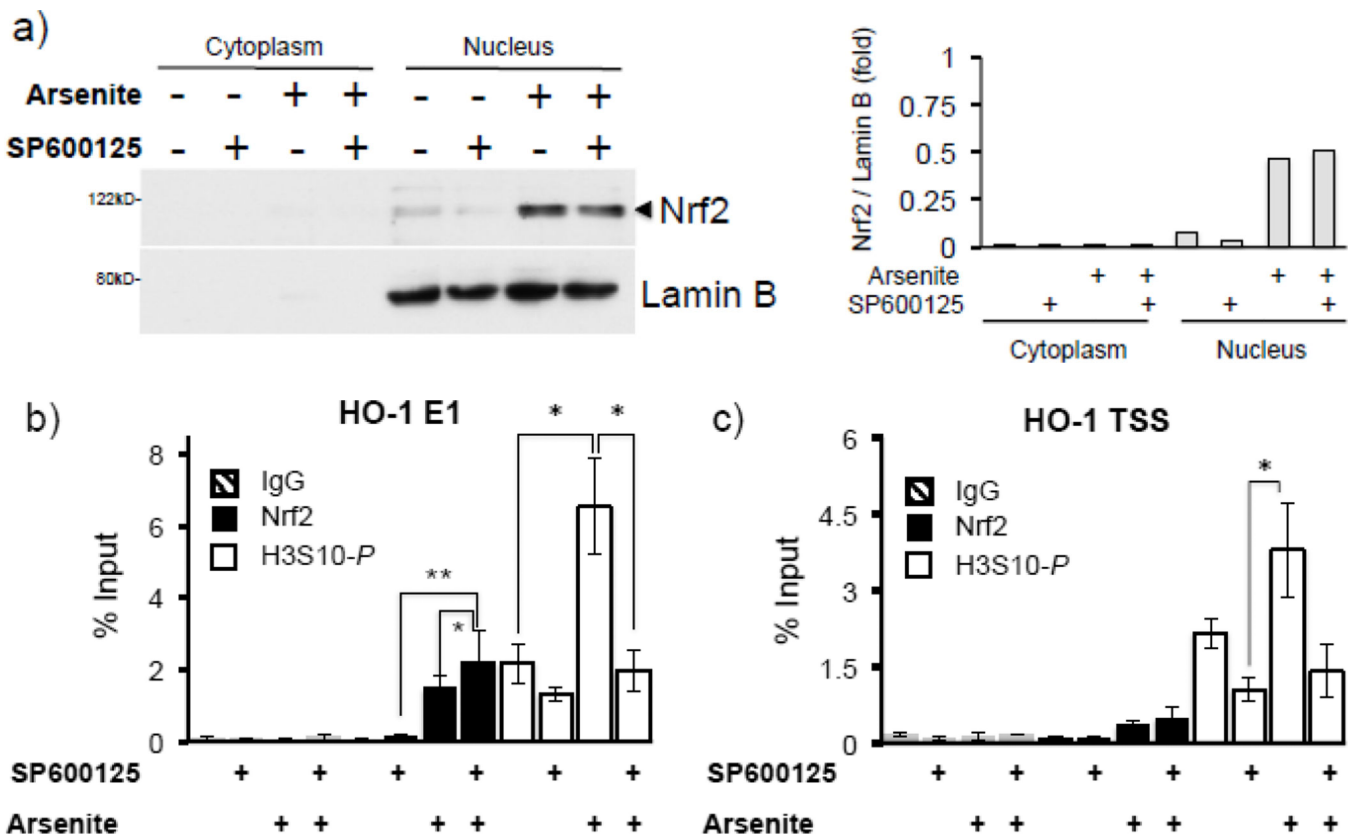
Figure 5. SP600125 inhibits enrichment of phosphorylated H3S10 but not Nrf2 on the HO-1 ARE in response to arsenite

(a) HaCaT cells were pretreated with 10μM SP600125 for 1 hr, then treated with 10μM arsenite for 4 hr and harvested as cytoplasmic and nuclear fractions and subjected to Western blot analysis with anti-Nrf2 specific antibodies; Lamin B blot is shown as loading control. Quantification of blots is shown to the right. Densitometry analysis was conducted with Image J software. Relative density of arsenite and SP600125 treated signal bands were normalized to the corresponding control signal bands for fold change, then further normalized to the relative density of Lamin B signal bands for loading accuracy. (b and c) HaCaT cells were pretreated with 10μM SP600125 for 1 hr, then treated with 10μM arsenite for 4 hr, harvested for chromatin immunoprecipitation (ChIP) and incubated with rabbit IgG, anti-H3S10 phospho-specific (H3S10-P), or anti-Nrf2 antibody. Isolated genomic DNA was subjected to quantitative RT-PCR using primer pairs for the HO-1 E1 (b) and TSS (c) regions. Samples were normalized to input and presented as percent input. Significance was calculated using a t-test and established with $p < 0.05$ (*) or $p < 0.01$ (**). A representative of three independent experiments is shown.
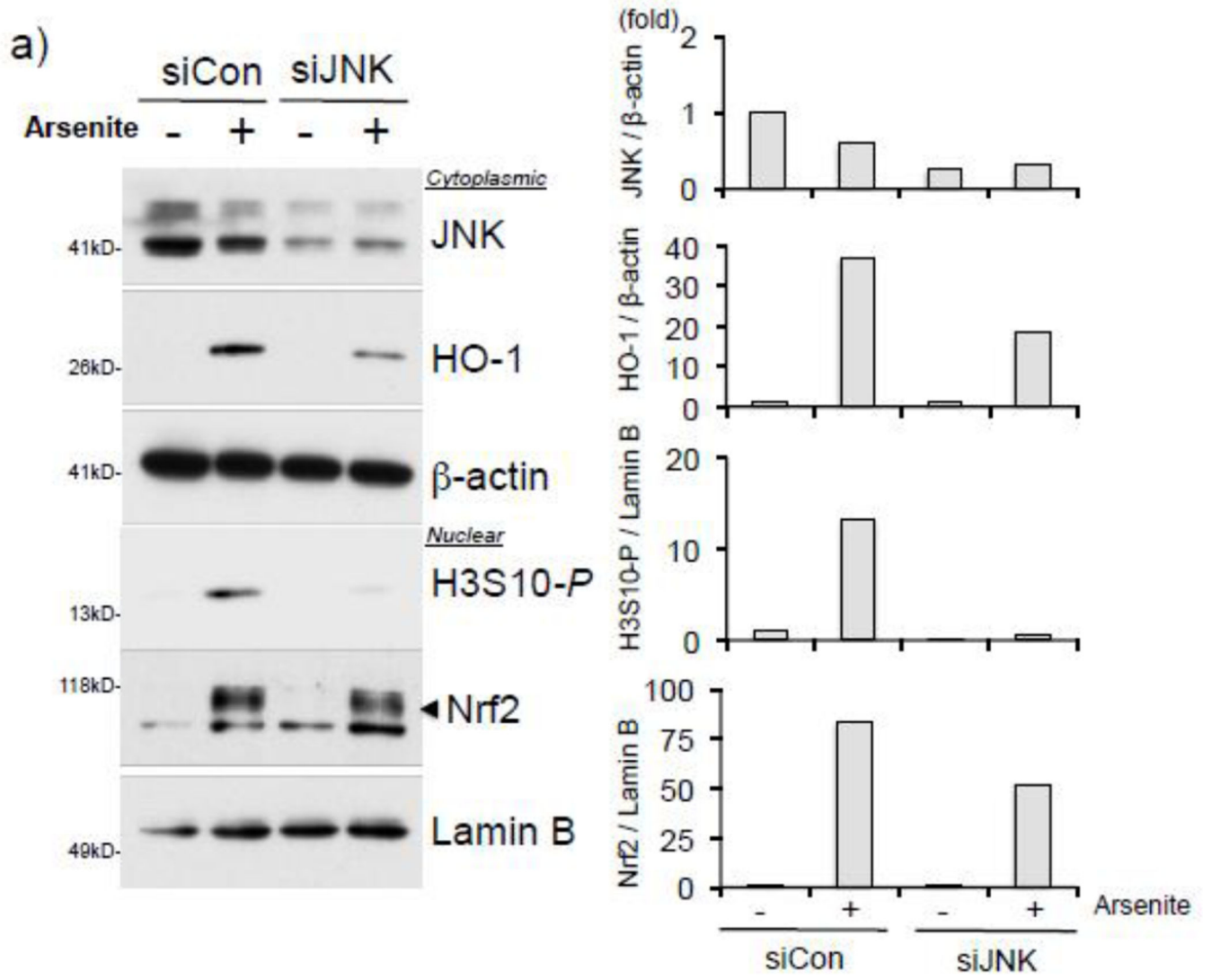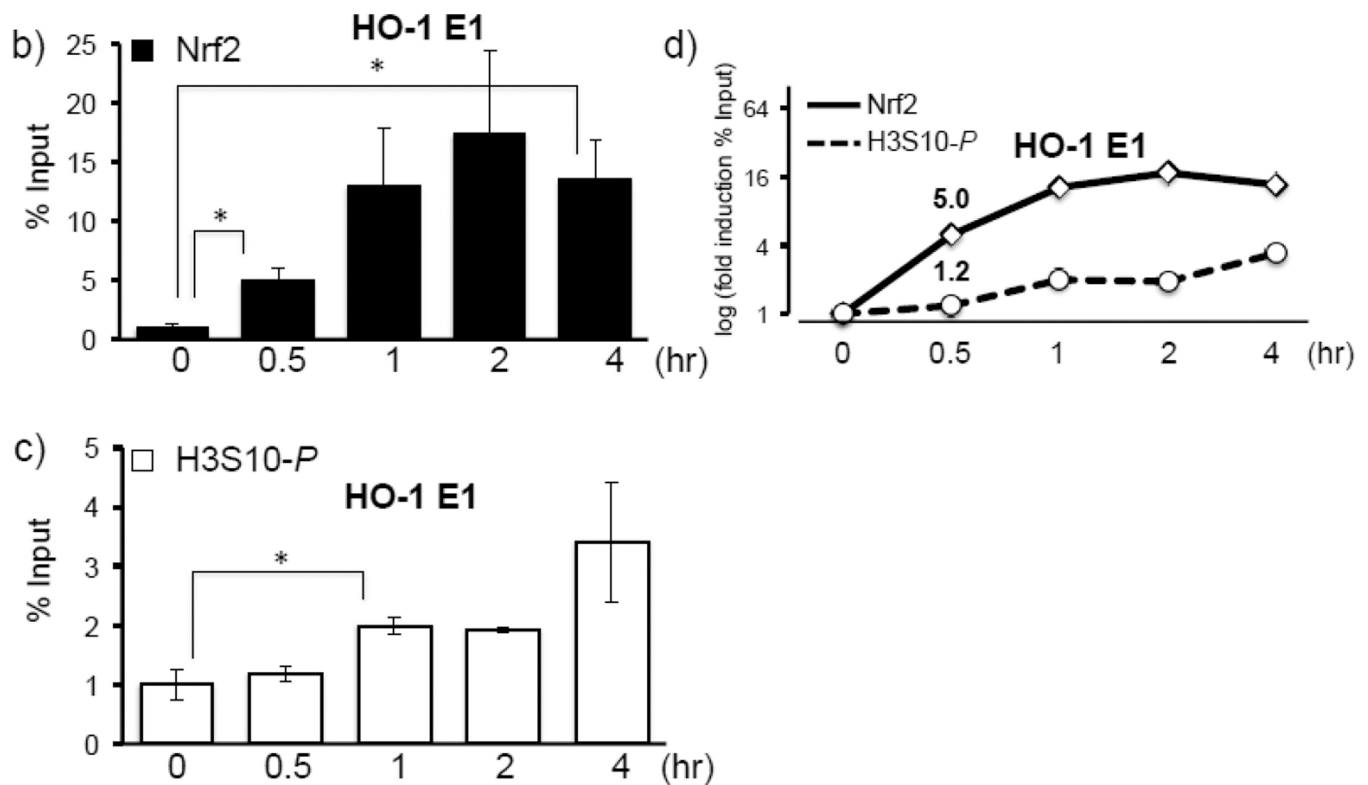
Figure 6. Arsenite induces JNK-dependent H3S10 phosphorylation and recruits Nrf2 to the HO-1 ARE prior to enrichment of phosphorylated H3S10

a) HaCaT cells were transiently transfected with JNK specific siRNA or control siRNA as described in Materials and Methods. After 48 hr, cells were treated with 10μM arsenite for 8 hr and nuclear and cytoplasmic fractions were subjected to Western blot analysis with anti-HO-1, anti-Nrf2, anti-JNK, and anti-H3S10 phospho-specific (H3S10-P) antibodies; Lamin B and β-Actin blots are shown as loading controls. Quantification of blots is shown to the right. Densitometry analysis was conducted with Image J software. Relative density of arsenite treated signal bands were normalized to the corresponding control signal bands (siCon/arsenite (−)) for fold change, then further normalized to the relative density of loading control signal bands for loading accuracy; JNK and HO-1 were normalized to β-Actin; H3S10-P and Nrf2 were normalized to Lamin B. (b and c) HaCaT cells were treated with 10μM arsenite for 0.5, 1, 2, or 4 hr, then harvested for ChIP assay and incubated with rabbit IgG, anti-Nrf2 (b), or anti-H3S10 phospho-specific (H3S10-P) (c) antibody. Isolated genomic DNA was subjected to quantitative RT-PCR using primer pairs for the HO-1 E1 region. Samples were normalized to input and presented as percent input. Significance was calculated using a t-test and established with $p < 0.05$. A representative of three independent experiments is shown. (d) Graphical representation of temporal induction of Nrf2 and phosphorylated H3S10 (H3S10-P) enrichment on the HO-1 E1 ARE.
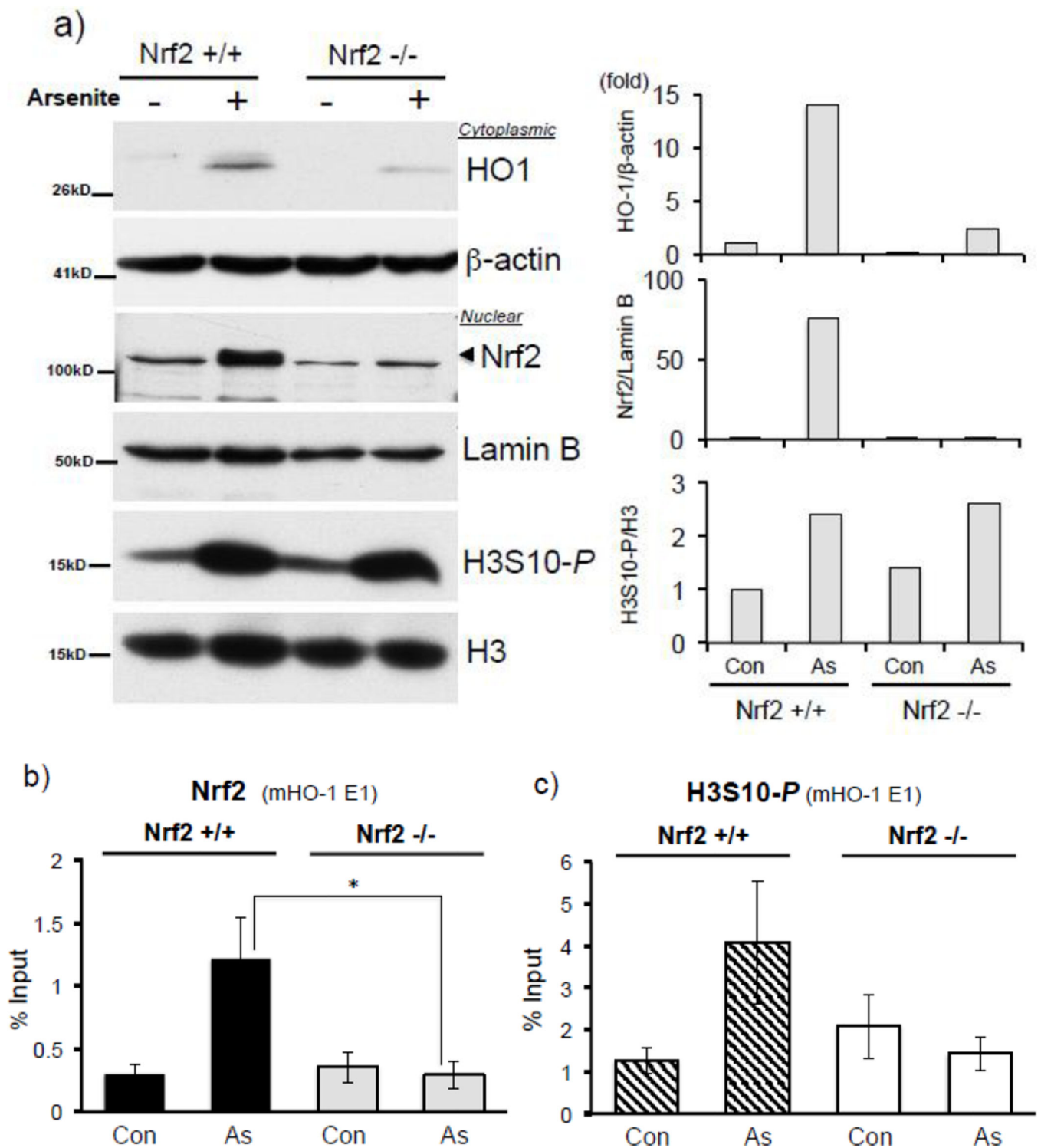
Figure 7. Nrf2 is associated with phosphorylation of H3S10 on the mouse Ho-1 ARE

a) Nrf2 +/+ and Nrf2 −/− MEF cells were treated with 10µM arsenite for 8 hr and nuclear and cytoplasmic fractions were subjected to Western blot analysis with anti-HO-1, anti-Nrf2, and anti-H3S10 phospho-specific (H3S10-P) antibodies; Lamin B, histone H3, and β-

Actin blots are shown as loading controls. Quantification of blots is shown to the right. Densitometry analysis was conducted with Image J software. Relative density of arsenite treated signal bands were normalized to the corresponding control signal bands (Nrf2+/+, arsenite (−)) for fold change, then further normalized to the relative density of loading control signal bands for loading accuracy; HO-1 was normalized to β-Actin; Nrf2 was normalized to Lamin B, and H3S10-P was normalized to H3. (b and c) Nrf2 +/+ and Nrf2 −/− MEF cells were treated with 10μM arsenite for 4 hr, harvested for ChIP assay, and incubated with rabbit IgG, (b) anti-Nrf2, or anti-H3S10 phospho-specific (H3S10-P) antibody. Isolated genomic DNA was subjected to quantitative RT-PCR using primer pairs for the mouse HO-1 E1 region. Samples were normalized to input and presented as percent input. Significance was calculated using a t-test and established with $p < 0.05$. A representative of three independent experiments is shown.